ELSEVIER

Surface and Coatings Technology 102 (1998) 90–96

SURFACE & COATINGS TECHNOLOGY

Effects of argon irradiation on a plasma-nitrided carbon steel

G. Simon, M.A.Z. Vasconcellos, C.A. dos Santos *

Instituto de Fisica — UFRGS Av. Bento Gonçalves, 9500, C.P. 15051 — Campus do Vale, 91501-970 Porto Alegre, RS, Brazil

Received 10 August 1997; accepted 20 October 1997

Abstract

We report on the effects of Ar irradiation on a plasma-nitrided steel. Samples of AISI 1010 steel were nitrided in a mixture of H_2-20% N_2 under a total pressure of 5 mbar. The current was adjusted to maintain the cathode temperature at 720 K. The nitrided samples were submitted to the following treatments: (a) Ar irradiation forming a plateau from near surface down to about 150 nm; (b) after each irradiation the samples were submitted to 1 h thermal annealing in high vacuum at temperatures between 523 and 973 K. X-ray diffraction and conversion electron Mössbauer spectroscopy measurements show that Ar irradiation induces the precipitation of finely dispersed ϵ-Fe_{2+x}(N,C), which are unstable at temperatures as low as 523 K. Further annealing at higher temperatures promotes the dissolution of the ϵ carbonitrides and increases the amount of γ'-Fe_4N, up to temperatures about 800 K, after which all the nitrides and carbonitrides are unstable. Our results show clearly that Ar bombardment can induce the transformation $\gamma' \rightarrow \epsilon_{3.2} + \epsilon_{2+x}$ which is consistent with the instability of small γ' precipitates at room temperature. © 1998 Elsevier Science S.A.

Keywords: Plasma nitriding; Argon irradiation; Mössbauer spectroscopy; X-ray diffraction

1. Introduction

Plasma nitriding, a widely accepted industrial process to improve mechanical and tribological properties of steels, has been used over the past 30 years [1,2], although the first patents were filed in the early 1930s [1,3]. On the other hand, ion implantation, as a nitriding technique, has been developed since the 1970s [4]. In addition to the studies concerning mechanical and tribological properties of different ion-implanted materials [5], several papers have been published about the chemical and structural modifications of the implanted surface [6–11], as well as the effect of post-bombardment with noble gases [12–17].

X-ray diffraction (XRD) analysis and metallography have shown [18,19] that the near-surface compound layer of plasma-nitrided steels consists mainly of ϵ-Fe_x(N, C) carbonitrides and γ'-Fe_4N nitride. ϵ_x comprise nitrides and carbonitrides with several stoichiometries, reported in the literature as ϵ-Fe_2(C, N), ϵ-Fe_{2+x}(C,N) ($x < 1.2$), ϵ-Fe_3(C, N) and ϵ-$Fe_{3.2}$(C, N), in the following designed simply ϵ_2, ϵ_{2+x}, ϵ_3 and $\epsilon_{3.2}$, respectively. Some authors have proposed the existence of the γ'-Fe_4(N, C) carbonitride in steels submitted to nitriding and nitrocarburizing [20], but because of the low carbon solubility in this nitride, it is very difficult to be sure of the existence of the γ' carbonitride, at least from XRD and Mössbauer measurements. In the following work we will only refer to the γ' nitride. Below the compound layer, there is the so-called diffusion zone, where the steel matrix is supersaturated by the in-diffusion nitrogen. Finely dispersed alloy nitride precipitates are also observed at the diffusion zone of alloy steels. Some studies have shown that the near-surface compound layer in plasma-nitrided steels consists of large precipitates [21].

Conversion electron Mössbauer spectroscopy (CEMS) and XRD measurements have shown that for nitrogen-implanted steels the situation is somewhat similar. The above nitrides and carbonitrides are also formed near the surface [6–11], but the thickness of the compound layer is at least one order smaller than that of the plasma-nitrided steels. The nitrides and carbonitrides formed in ion-implanted carbon steels are unstable under annealing in high vacuum at temperatures as low as 523 K; at about 750 K, there are no precipitates in the near-surface region [8]. Instability at such low temperatures can be due to finely dispersed precipitates.

This is a significant difference regarding the post-

* Corresponding author: Tel: 0055 51 316 6424; Fax: +55 51 319 1762; e-mail: cas@if.ufrgs.br

PII S0257-8972(97)00691-9

bombardment studies because during irradiation some coarsening of small precipitates can occur, while large precipitates will shrink to the equilibrium size [22,23]. Therefore, the behavior of ion-implanted and plasma-nitrided samples after the post-bombardment is expected to be noticeably different. The effects of post-bombardment on nitrogen-implanted carbon steels have been studied at length in the last decade [12–17]. He, Ar, Kr and Xe have been used as the bombarding ion. These studies have shown two main effects produced by every ion: (1) dissolution and reprecipitation of the carbonitrides formed during N-implantation; and (2) rise of the temperature for complete dissolution of the precipitates.

To qualitatively consider the role of the precipitates size on the results discussed above, we have performed the present study on the effects of Ar bombardment on a plasma-nitrided carbon steel. The experimental design was chosen in order to compare our results with those previously published about the effects of noble gases bombardment on N-implanted steels [12–17].

2. Experimental details

Samples from the same ingot of commercial low carbon steel (AISI 1010, in wt.%: 0.11 C, 0.39 Mn, 0.18 Cr, 0.23 Ni) were mirror polished and nitrided in an equipment similar to one described by Hudis [2]. Nitriding was performed for 15 min (sample A15), 30 min (sample A30) and 60 min (sample A60). A mixture of H_2 and 20% N_2 under a total pressure of 5 mbar, submitted to 750 V, was used for all samples. The current was adjusted to maintain the cathode temperature at 720 K, which was measured by a chromel–alumel thermocouple embedded in the sample.

After nitriding, the samples were cooled in the treatment chamber, with a nitrogen atmosphere, and submitted to the following treatments: (a) thermal annealing in high vacuum ($P \cong 5 \times 10^{-7}$ mbar) at temperatures between 523 and 973 K for 1 h; and (b) room temperature Ar irradiation (samples A15Ar, A30Ar and A60Ar) by using the 400 kV ion implanter at the Institute of Physics, Porto Alegre, forming a plateau from the near-surface down to about 150 nm. Following the TRIM (transport of ions in matter) predictions [24] this plateau can be obtained by sequential bombardment of Ar^+ at 50, 100 and 150 keV. To be compared with previous works [12–17] fluences around 10^{15} Ar/cm^2 were used, and the current densities were kept at about 1 μA/cm^2 in order to avoid heating of the samples. The irradiated samples were submitted to thermal annealing as described above.

XRD measurements, in θ–2θ geometry and in glancing angle geometry with incidence angle $\alpha = 5^\circ$, were carried out in a Siemens diffractometer with monochromated CuKα radiation ($\lambda = 0.1542$ nm). This incidence angle was chosen because it enable us to probe exclusively the compound layer, without any signal of the steel matrix, for any nitriding time used. All the XRD patterns were obtained with a scan step of $0.05^\circ 2\theta$ in the range from 5° to 100°, with a fixed counting time of 2 s.

The Mössbauer spectroscopy data were obtained in a backscattering geometry. A proportional flow counter with He and 5% CH_4 (for CEMS) or Ar and 5% CH_4 (for CXMS), was used with a conventional constant-acceleration Mössbauer spectrometer. The source was ^{57}Co in an Rh matrix with a nominal activity of 50 mCi. All the CEMS and CXMS measurements were performed at room temperature. The hyperfine parameters were obtained by a least-squares procedure assuming Lorentzian line shapes. Isomer shifts are given relative to α-Fe at RT.

3. Results

3.1. The as-nitrided samples

Fig. 1 shows θ–2θ XRD patterns for the samples nitrided for 15, 30 and 60 min. The diffratogram displayed in Fig. 1a shows reflections from the steel matrix, the γ' nitride and the ϵ_x carbonitrides. As the nitriding time increases, the intensities of the reflections attributed to the steel matrix and to ϵ_x carbonitrides decrease. For the nitriding time $t = 60$ min, Fig. 1c, there is no signal

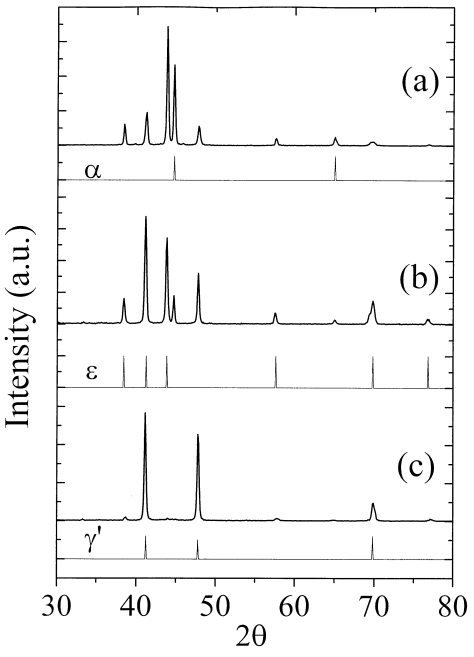

Fig. 1. θ–2θ XRD diffractograms for AISI-1010 sample nitrided for: (a) 15 min (sample A15); (b) 30 min (sample A30); and (c) 60 min (sample A60).

of the steel matrix. The corresponding CEMS spectra are shown in Fig. 2.

The CEMS spectra were fitted by the addition of subspectra corresponding to α_N (the matrix component), to ϵ_x with different stoichiometries and to γ'. Typical hyperfine parameters used to fit these spectra are displayed in Table 1. These parameters are similar to those previously published [8–13,25–28]. Table 2 and Fig. 3 show the relative spectral areas obtained from these fittings. For the smaller nitriding time, $t=15$ min, the CEMS spectrum consists of 7% of α_N, 55% of $\epsilon_{3.2}$, and 38% of γ'. Nitriding for 30 min increases the amount of $\epsilon_{3.2}$ up to 64%, mostly at the expense of that corresponding to γ'. For the sample nitrided with $t=60$ min there is a remarkable increase in the area attributed to γ', at the expense of that attributed to $\epsilon_{3.2}$. This spectrum was fitted with 5% of α_N, 4% of $\epsilon_{3.2}$ and 91% of γ'. The CXMS spectra for these same samples show a similar trend [29].

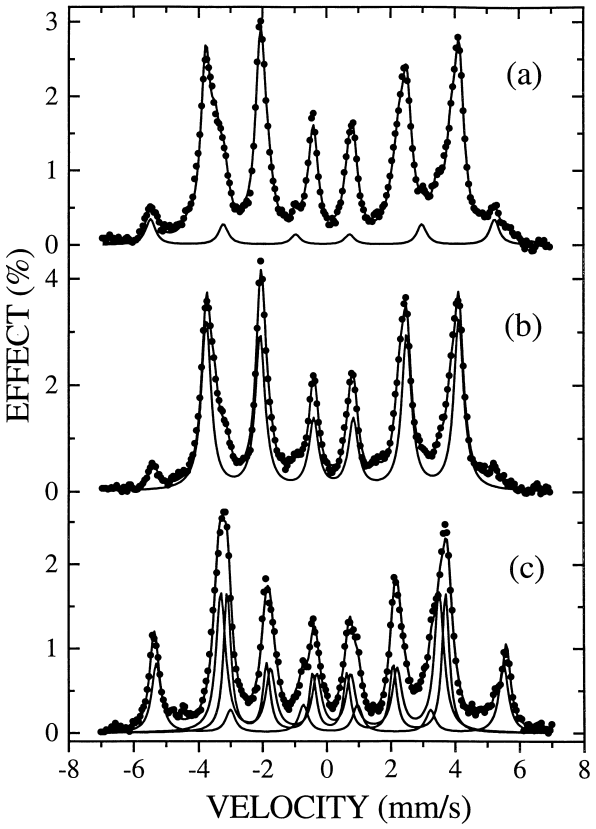

Fig. 2. CEMS spectra for the samples described in Fig. 1. The subspectra attributed to α_N, $\gamma_{3.2}$ and γ' are shown, respectively, in (a), (b) and (c).

Table 1
Typical values of the parameters used to fit the different ^{57}Fe CEMS and CXMS spectra shown in this work. The isomer shifts are given relative to α-Fe. Typical errors are: ±3%

Component	H (kG)	ΔE_Q (mm s^{-1})	δ (mm s^{-1})
Steel matrix	331	0.01	0.01
ϵ-$Fe_{3.2}$(C, N)	290	0.02	0.29
	243	0.29	0.21
ϵ-Fe_{2+x}(C, N) $x<1.2$	285	0.21	0.02
	220	0.21	0.12
	90	0.41	0.11
γ'-Fe_4N	338	0.21	0.21
	210	0.31	0.09

3.2. The as-irradiated samples

GXRD diffractograms of the nitrided samples submitted to argon irradiation suggest the relative increase of the ϵ carbonitrides for all the samples. However, this result is more clearly displayed for the sample A60Ar (Fig. 4a) because of the very small concentration of these carbonitrides in the as-nitrided sample. More drastic modifications are observed in the CEMS spectra, for all the samples after Ar irradiation. As can be seen in Table 2 and Fig. 5a, a considerable increase has been observed on the proportion of carbonitrides, which are satisfactorily discriminated by CEMS and CXMS, but not by XRD. The CEMS spectrum of the A15Ar sample was fitted to 18% of α_N, 26% of γ', 19% of $\epsilon_{3.2}$ and 37% of ϵ_{2+x}. For A30Ar the fitting resulted in 11% of α_N, 29% of γ', 20% of $\epsilon_{3.2}$ and 40% of ϵ_{2+x}, while for A60Ar we have obtained 3% of α_N 24% of γ', 22% of $\epsilon_{3.2}$ and 51% of ϵ_{2+x}. The comparison between the CEMS and CXMS results show that after Ar irradiation the ϵ_x compounds precipitate in the very near-surface region. For the sample A60Ar, the ratio between the CEMS and CXMS areas increase notably for α_N and γ', and decrease for ϵ_{2+x} and $\epsilon_{3.2}$. The decrease is more appreciable for ϵ_{2+x} so that this is the nearest-surface compound formed after Ar bombardment.

The most prominent effect of the argon bombardment is the precipitation of ϵ_{2+x} carbonitrides, not present in the as-nitrided samples. Table 2 shows that for the as-implanted samples, the CEMS spectral area increases for ϵ_{2+x}, and decreases for α_N, as a function of the nitriding time. The γ' and $\epsilon_{3.2}$ CEMS spectral areas remain almost constant. Other interesting features can be highlighted by using the CEMS area increment, defined as the difference between the relative areas after and before Ar irradiation. These differences are shown, as a function of the nitriding time, in Fig. 6. The ϵ_{2+x} increase and the α_N decrease are displayed, but more interesting are the significant variations of γ' and $\epsilon_{3.2}$ CEMS areas increment, whose evolution is the opposite of that showed in Fig. 3, for the as-nitrided samples.

3.3. Thermal evolution of Ar-irradiated samples

The annealing results of the as-nitrided samples [29] show that the compound layer is stable up to 773 K. Below this temperature there are no significant changes

Table 2
Relative CEMS and CXMS spectral areas: as-nitrided and as-implanted samples. Typical errors are ±5%

Sample	Steel matrix CEMS/CXMS	γ' CEMS/CXMS	$\epsilon_{3.2}$ CEMS/CXMS	ϵ_{2+x} ($x<1.2$) CEMS/CXMS
A15	7/75	38/10	55/15	0/0
A15Ar	18/80	26/8	19/5	37/7
A30	6/57	30/24	64/19	0/0
A30Ar	11/62	29/22	20/6	40/10
A60	5/46	91/52	4/2	0/0
A60Ar	3/35	24/41	22/15	51/9

on the XRD patterns or on the CEMS and CXMS spectra. Matrix XRD reflections are present only after annealing at temperatures higher than 773 K. For the Ar-irradiated samples the results are different to a large extent.

The GXRD patterns for the A60 sample submitted to Ar irradiation and annealed at 523, 593 and 773 K are shown in Fig. 4. As detected by GXRD, the implanted layer is significantly changed only after annealing at 773 K. However, Fig. 5b shows that CEMS detect modifications after annealing at 523 K. General outlooks of the thermal evolution of the Ar bombarded samples, as measured by CEMS, are displayed in Figs. 7–9 and in Table 3.

For the sample A15Ar (Fig. 7) annealed at 523 K, a significant increase of $\epsilon_{3.2}$ at the expense of α_N and ϵ_{2+x} was observed. The relative area attributed to γ' remains equal to 26%. Subsequent annealings decrease the ϵ_{2+x} contribution continuously. Other interesting features are noticeable for the evolution of the spectral areas from α_N, γ', and $\epsilon_{3.2}$. Annealing at 593 K induces the growth of the γ' spectral area and the reduction of that attributed to $\epsilon_{3.2}$. Further annealing (673 K) shows considerable increase of the α_N relative concentration and the decrease of those corresponding to the other components. For the sample A30Ar (Fig. 8) the thermal evolution is somewhat different. For annealing at temperatures higher than 523 K, the relative contribution from ϵ_{2+x}, remains almost constant, those from α_N and γ' increase and that from $\epsilon_{3.2}$ decrease. Therefore, compared with A15Ar, the behavior of γ' shows the most important discrepancy, although the rate of decrease of the contribution from $\epsilon_{3.2}$ has increased considerably. For the sample A60Ar, the Fig. 9 clearly indicates a tendency for the compound layer recovery before thermal dissolution of the precipitates, which occurs for annealing temperatures higher than 800 K.

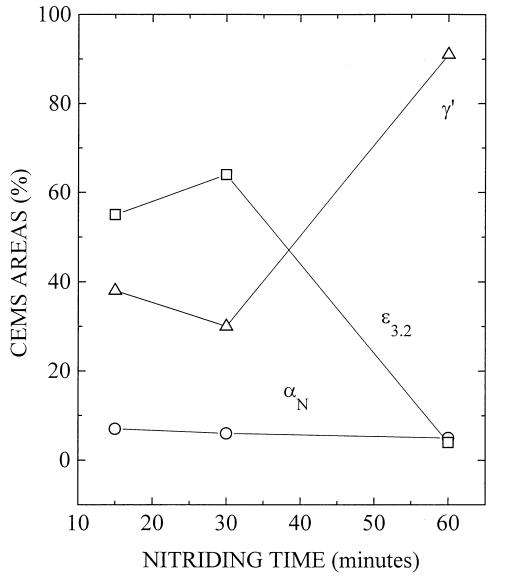

Fig. 3. Relative concentration of nitride and carbonitride precipitates as a function of nitriding time, obtained from the spectra shown in Fig. 2. The solid lines are guide to the eyes.

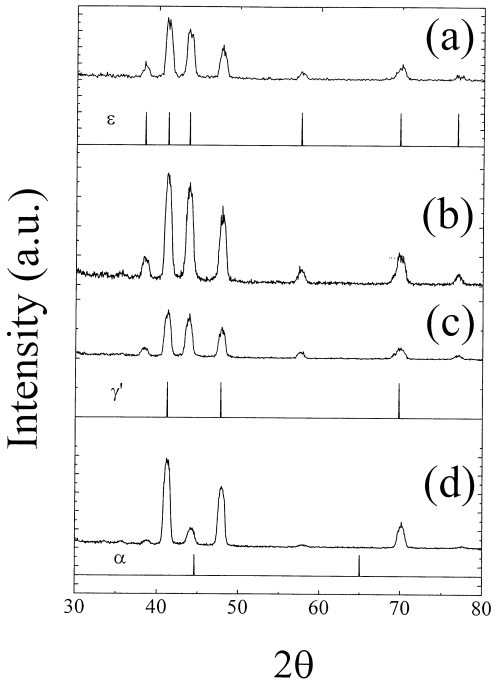

Fig. 4. GXRD diffractograms, with $\alpha=5°$, for: (a) sample A60 implanted with Ar (sample A60Ar); (b) sample A60Ar annealed at 523 K; (c) sample A60Ar annealed at 593 K; and (d) sample A60Ar annealed at 773 K.

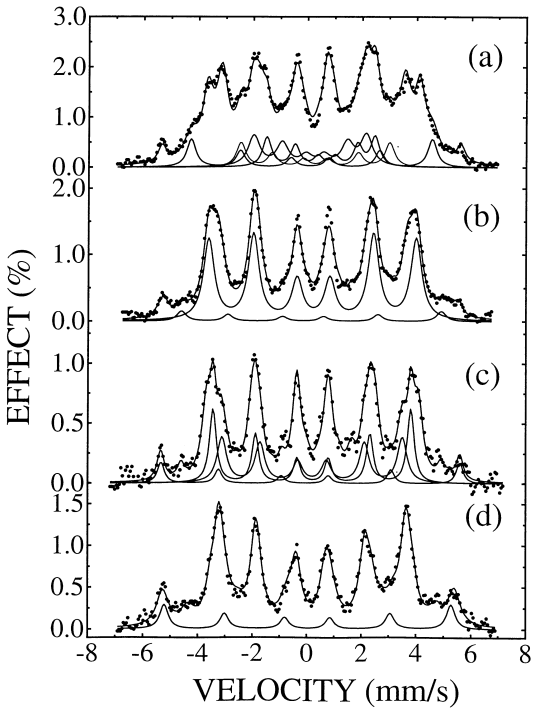

Fig. 5. CEMS spectra for the samples described in Fig. 4. The subspectra attributed to ϵ_{2+x}, $\epsilon_{3.2}$, γ' and α_N are shown, respectively, in (a), (b), (c) and (d).

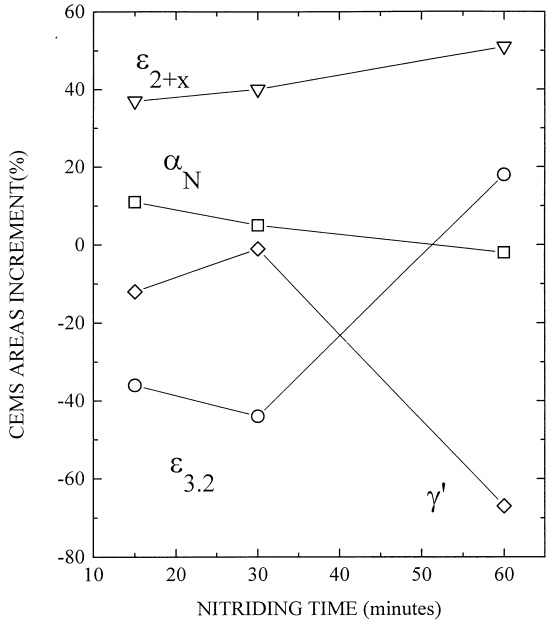

Fig. 6. Difference between the CEMS areas before and after Ar irradiation. The solid lines are guide to the eyes.

4. Discussion

Regarding the chemical composition of the compound layer as well as the precipitates volume, the three samples prepared by plasma nitriding are different. As shown in Fig. 3, the samples A15 and A30 are almost identical,

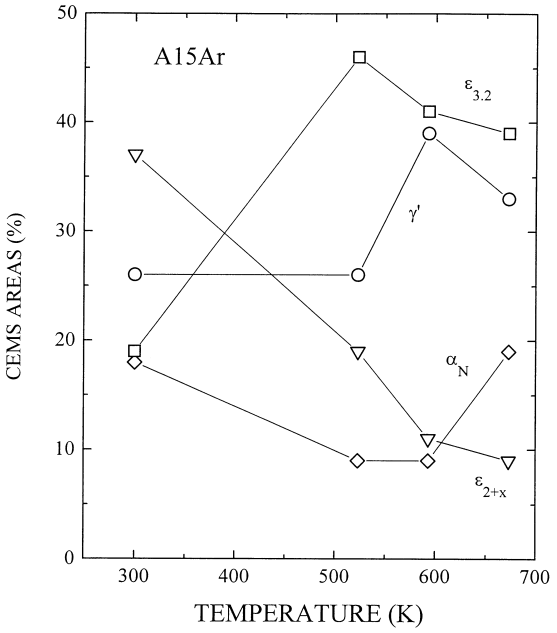

Fig. 7. Relative concentrations of nitride and carbo nitride precipitates as a funcion of the temperature of annealing, obtained from the CEMS spectra for sample A15Ar. The solid lines are a guide to the eyes.

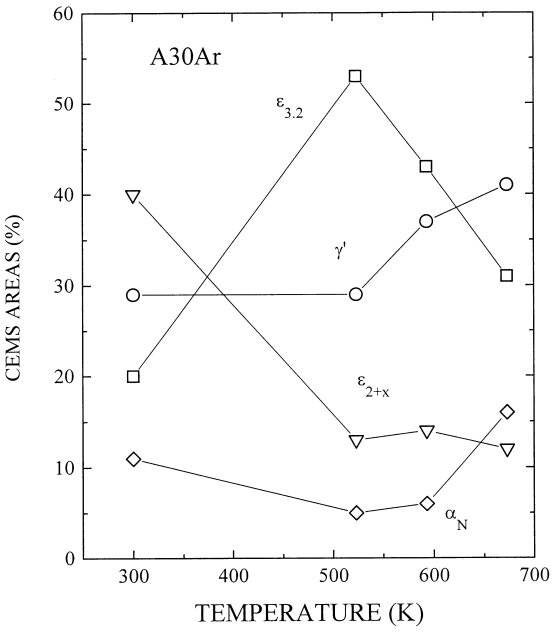

Fig. 8. Relative concentrations of nitride and carbo nitride precipitates as a funcion of the temperature of annealing, obtained from the CEMS spectra for sample A30Ar. The solid lines are a guide to the eyes.

but quite different from the A60 one, as the near-surface chemical composition is concerned. The latter sample contains essentially γ' precipitates, while significant amounts of γ' and $\epsilon_{3.2}$ are present in the former samples. As demonstrated for gas-nitrided steels [30], it is expected the growth of the precipitates as a function of the nitriding time, for the plasma-nitrided carbon steels. Taking this picture into account, we will compare our

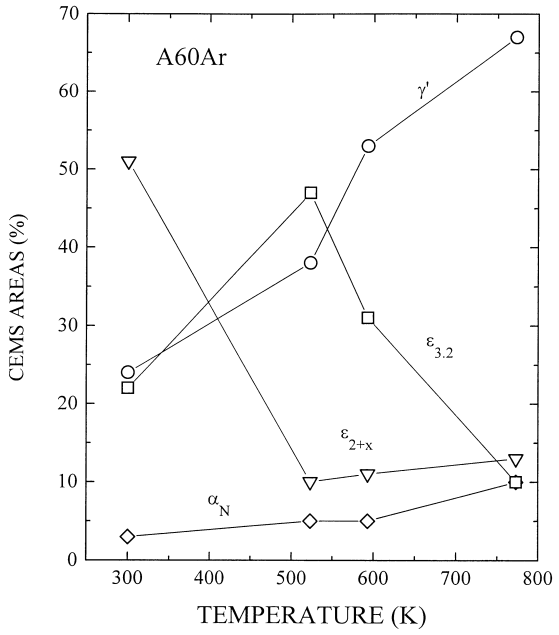

Fig. 9. Relative concentrations of nitride and carbo nitride precipitates as a funcion of the temperature of annealing, obtained from the CEMS spectra for sample A60Ar. The solid lines are a guide to the eyes.

results with those previously published for noble gases bombardment on N-implanted carbon steels [12–17].

The results displayed in Fig. 6 allow us to assume that for the A15Ar and A30Ar samples, the increase of the α_N relative concentration is mainly due to the decrease of that of γ', while the precipitation of ϵ_{2+x} is correlated to the dissolution of $\epsilon_{3.2}$. The nitrogen and carbon required for the more rich ϵ_{2+x} comes from the partial dissolution of γ' and from the supersatured steel matrix. Partial transformation of γ' into α_N has been reported for an N-implanted iron bombarded by He [12], whereas dissolution of $\epsilon_{3.2}$ and reprecipitation of ϵ_{2+x} has been reported for Ar, Kr and Xe bombardment on N-implanted carbon steels [13,15–17]. From the results above, the $\gamma' \rightarrow \alpha_N$ transformation on A60Ar would be expected. However, it was observed the partial transformation of γ' into ϵ_{2+x} and $\epsilon_{3.2}$.

According to Nelson et al. [22], the stability of precipitates under irradiation depends on the balance between the radiation dissolution of precipitates and their growth by irradiation enhanced and thermal diffusion. When an alloy containing precipitates is subjected to irradiation, the new equilibrium condition is attained by the precipitates changing their size, so that some coarsening of small precipitates and shrinking of large ones can occur to reach the equilibrium size. This kind of phenomena has been observed in the dissolution of nitride precipitates in iron by low-dose neutron irradiation [23]. Previous results on N-implanted iron, bombarded with He ions [12] can also be understood in this context. The noble gas bombardment induces a coarsening of the small precipitates formed during the nitrogen implantation. Because of this coarsening, the precipitates becomes slightly more stable under thermal activation. On the other hand, when the as-implanted iron sample is first annealed at 673 K, enlarging of the γ' precipitates can occur. The subsequent He bombardment will shrink these precipitates, which become less stable [12].

Taking the discussion above into account, we propose the following explanation for the results reported here. During Ar bombardment of the samples A15Ar and A30Ar, large precipitates are eroded from the perimeter inwards, in a similar way as previously suggested [23]. The nitrogen liberated diffuses in the matrix, in which it can be trapped by defects or recombines with the original large precipitates. After the bombardment the nitrogen-point-defect complexes provide the nuclei for small ϵ_{2+x} precipitates. These small precipitates are readily dissolved after annealing at temperatures as low as 523 K. Figs. 7–9 suggest that some of these ϵ_{2+x} carbonitrides reprecipitate during the cooling process. It is reasonable to suppose that thermal dissolution and reprecipitation during the cooling process also occur for the other nitrides and carbonitrides.

The most striking result illustrated here is the transformation $\gamma' \rightarrow \epsilon_{3.2} + \epsilon_{2+x}$ under Ar irradiation on the sample A60Ar. Similar results have also been observed in N-implanted iron submitted to annealing and Ar bombardment [31]. The dissolution of large precipitates in A60Ar resembles that proposed for A15Ar and

Table 3
Relative CEMS and CXMS spectral areas: implanted samples submitted to thermal annealing. Typical errors are ±5%

Sample T (K)		Steel matrix CEMS/CXMS	γ' CEMS/CXMS	$\epsilon_{3.2}$ CEMS/CXMS	ϵ_{2+x} ($x<1.2$) CEMX/CXMS
A15Ar	523	9/67	26/20	46/7	19/6
	593	9/72	39/15	41/7	11/6
	673	19/72	33/16	39/7	9/5
A30Ar	523	5/61	29/24	53/9	13/6
	593	6/60	37/25	43/10	14/5
	673	16/67	41/20	30/9	12/4
A60Ar	523	5/38	38/45	47/13	10/4
	593	5/38	53/46	31/12	11/4
	773	10/36	67/60	10/4	13/0

A30Ar. The small precipitates resulting from the γ' dissolution would be expected to have the γ' stoichiometry. However, Vredenberg et al. have suggested that γ' becomes unstable below 583 K [32]. Therefore, the $\gamma' \rightarrow \epsilon_{3.2} + \epsilon_{2+x}$ transformation indicates that the above prediction can be realized for small precipitates. The nitrogen required for achieve the ϵ stoichiometry comes from the supersatured matrix, presumably promoted by radiation-enhanced diffusion.

The thermal behavior of our samples is consistent with the discussion above. The impressive dissolution of ϵ_{2+x} is a clear indication of finely dispersed precipitates. Similar results have been observed firstly in N-implanted carbon steel [9] and after confirmed in N-implanted iron [33]. In both kind of samples, thermal stability is improved by increasing the implanted nitrogen dose. For instance, the precipitates formed on AISI-1020 carbon steel implanted with 4×10^{17} N^+ ion cm^{-2} decompose at temperatures about 523 K, while those formed on the same material implanted with 6×10^{17} N^+ ion cm^{-2} decompose at temperatures about 593 K [9].

5. Conclusions

The high thermal stability of the plasma-nitrided low carbon steels is connected to the large volume of the iron carbonitrides precipitates. Ar irradiation induces the precipitation of finely dispersed ϵ_{2+x} carbonitrides, which are unstable at temperatures as low as 523 K. Further annealing at higher temperatures promote the transformation $\epsilon \rightarrow \alpha_N + \gamma'$, up to temperatures about 800 K, after which all the nitrides and carbonitrides are unstable. Our results clearly show that Ar bombardment can induce the transformation $\gamma' \rightarrow \epsilon_{3.2} + \epsilon_{2+x}$, which is consistent with the instability of small γ' precipitates at room temperature.

Acknowledgement

We thank to Drs L. Amaral and L.F. Ziebell for valuable comments on this manuscript. This work was partially supported by the Brazilian agencies CNPQ, FAPERGS, FINEP and CAPES.

References

[1] T. Bell, Surf. Engng 6 (1990) 31.
[2] M. Hudis, J. Appl. Phys. 44 (1973) 1489.
[3] P.C. Jindal, J. Vac. Sci. Technol. 15 (1978) 313.
[4] N.E.W. Hartley, G. Deamaley, J.F. Turner, J. Saunders, in: S.T. Picraux, E.P. Eer Nisse, F.L. Vook (Eds.), Applications of Ion Beams to Metals, Plenum, New York, 1974, p. 123.
[5] H. Hennan, Nucl. Instrum. Method. 182183 (1981) 887.
[6] G. Principi, P. Matteazzi, E. Ramous, G. Longworth, J. Mater. Sci. 15 (1980) 2665.
[7] D. Firrao, M. Rosso, G. Principi, R. Frattini, J. Mater. Sci. 17 (1982) 1773.
[8] C.A. dos Santos, de BarrosB.A.S., Jr, J.P. de Souza, I.J.R. Baumvol, Appl. Phys. Lett. 41 (1982) 237.
[9] C.A. dos Santos, M. Behar, I.J.R. Baumvol, J. Phys. D: Appl. Phys. 17 (1984) 551.
[10] N. Moncoffre, Mater. Sci. Engng 90 (1987) 99.
[11] G. Marest, Defect Diffusion Forum 535455565758 (1988) 273.
[12] M. Behar, P.J. Viccaro, M.T.X. Silva, A. Vasquez, C.A. dos Santos, F.C. Zawislak, Nucl. Instrum. Method. B 1920 (1987) 132.
[13] S.M.M. Ramos, L. Amaral, M. Behar, G. Marest, A. Vasquez, F.C. Zawislak, Radiat. Effects Defects Solids 110 (1989) 355.
[14] S.M.M. Ramos, L. Amaral, M. Behar, G. Marest, A. Vasquez, F.C. Zawislak, J. Phys.: Condens. Matter 1 (1989) 8799.
[15] S.M.M. Ramos, L. Amaral, M. Behar, M. Brunel, G. Marest, M.A. Elkhakani, N. Moncoffre, J. Tousset, A. Vasquez, F.C. Zawislak, Appl. Phys. A 51 (1990) 476.
[16] M. Behar, L. Amaral, S.M.M. Ramos, A. Vasquez, F.C. Zawislak, J. Appl. Phys. 68 (1990) 4487.
[17] C.E. Foerster, L. Amaral, N. Moncoffre, M. Behar, Appl. Phy. A 54 (1992) 225.
[18] B. Edenhofer, Heat Treat. Metals 1 (1974) 23.
[19] B. Edenhofer, Heat Treat. Metals 1 (1974) 59.
[20] M.A.J. Somers, E.J. Mittemeijer, Metall. Trans. A 21 (1990) 189.
[21] J. Michalski, Surf. Coat. Technol. 59 (1993) 321.
[22] R.S. Nelson, J.A. Hudson, D.J. Mazey, J. Nucl. Mater. 44 (1972) 318.
[23] I.M. Robertson, C.A. English, M.L. Jenkins, Radiat. Effects 102 (1987) 53.
[24] J.P. Biersack, L.G. Haggmark, Nucl. Instrum. Meth. 174 (1980) 257.
[25] K.H. Eickel, W. Pitsch, Phys. Stat. Sol. 39 (1970) 121.
[26] A.J. Nozik, WoodJ.C., Jr, G. Haacke, Solid State Commum. 8 (1970) viii.
[27] G. Le Caer, A. Lorenzo, J.M. Génin, Phys. Status Sol. A 6 (1971) K97.
[28] N. DeCristofaro, R. Kaplow, Metall. Trans. A. 8 (1977) 35.
[29] G. Simon, M.Sc. Dissertation (unpublished), Institute of Physics, Federal University of Rio Grande do Sul, 1995.
[30] B. Mortimer, P. Grievson, K.H. Jack, Scand. J. Metall. 1 (1972) 203.
[31] C.E. Foerster, Ph.D. Thesis (unpublished), Institute of Physics, Federal University of Rio Grande do Sul, 1994.
[32] A.M. Vredenberg, C.M. Pérez-Martin, J.S. Custer, D.O. Boema, L. de Wit, F.W. Saris, N.M. van der Pers, Th.H. de Keijser, E.J. Mittemeijer, J. Mater. Res. 7 (1992) 2689.
[33] M. Kopcewicz, J. Jagielski, A. Turos, D.L. Williamson, J. Appl. Phys. 71 (1992) 4217.